Clinical Cancer Research

Combination Therapy with NHS-muIL12 and Avelumab (anti-PD-L1) Enhances Antitumor Efficacy in Preclinical Cancer Models

Chunxiao Xu, Yanping Zhang, P. Alexander Rolfe, Vivian M. Hernández, Wilson Guzman, Giorgio Kradjian, Bo Marelli, Guozhong Qin, Jin Qi, Hong Wang, Huakui Yu, Robert Tighe, Kin-Ming Lo, Jessie M. English, Laszlo Radvanyi, and Yan Lan

Abstract

Purpose: To determine whether combination therapy with NHS-muIL12 and the anti-programmed death ligand 1 (PD-L1) antibody avelumab can enhance antitumor efficacy in preclinical models relative to monotherapies.

Experimental Design: BALB/c mice bearing orthotopic EMT-6 mammary tumors and μMt$^-$ mice bearing subcutaneous MC38 tumors were treated with NHS-muIL12, avelumab, or combination therapy; tumor growth and survival were assessed. Tumor recurrence following remission and rechallenge was evaluated in EMT-6 tumor-bearing mice. Immune cell populations within spleen and tumors were evaluated by FACS and IHC. Immune gene expression in tumor tissue was profiled by NanoString® assay and plasma cytokine levels were determined by multiplex cytokine assay. The frequency of tumor antigen–reactive IFNγ-producing CD8$^+$ T cells was evaluated by ELISpot assay.

Results: NHS-muIL12 and avelumab combination therapy enhanced antitumor efficacy relative to either monotherapy in both tumor models. Most EMT-6 tumor–bearing mice treated with combination therapy had complete tumor regression. Combination therapy also induced the generation of tumor-specific immune memory, as demonstrated by protection against tumor rechallenge and induction of effector and memory T cells. Combination therapy enhanced cytotoxic NK and CD8$^+$ T-cell proliferation and T-bet expression, whereas NHS-muIL12 monotherapy induced CD8$^+$ T-cell infiltration into the tumor. Combination therapy also enhanced plasma cytokine levels and stimulated expression of a greater number of innate and adaptive immune genes compared with either monotherapy.

Conclusions: These data indicate that combination therapy with NHS-muIL12 and avelumab increased antitumor efficacy in preclinical models, and suggest that combining NHS-IL12 and avelumab may be a promising approach to treating patients with solid tumors. *Clin Cancer Res; 23(19); 5869–80. ©2017 AACR.*

Introduction

Tumor cells often exploit normal physiologic pathways to evade immune surveillance. Programmed death ligand 1 (PD-L1) is commonly upregulated in various tumors and tumor-infiltrating immune cells (1) and promotes a host of immunosuppressive effects upon binding to its receptor, programmed death 1 (PD-1), or to the costimulatory molecule CD80 (B7.1). These effects include stimulating the development of regulatory T cells (Treg; refs. 1, 2), promoting the exhaustion and apoptosis of activated T cells (3), and preventing the priming and activation of CTLs and their recruitment to the tumor (4).

Blockade of the PD-1/PD-L1 pathway can inhibit these immunosuppressive effects, thereby restoring the endogenous antitumor immune response. In the clinic, immunotherapies targeting PD-1/PD-L1 have been effective in inducing durable, complete responses in a subset of patients (5–9). However, many patients do not benefit from treatment due to resistance to anti-PD-1/PD-L1 therapies. Although molecular mechanisms of intrinsic resistance are complex and vary by indication, one important mechanism occurs through the lack of immune cell infiltration in the tumor, which is associated with poor prognosis and predicts an incomplete response to immunotherapy (10). Thus, combination of anti-PD-1/PD-L1 with other immunomodulators promoting immune cell infiltration into the tumor microenvironment is a rational strategy to overcome resistance and improve therapeutic responses.

One such therapeutic agent is the proinflammatory cytokine IL12, which plays a critical role in regulating the transition from innate to adaptive immunity. IL12 is released locally by activated phagocytes and dendritic cells during T-cell priming (11) and acts directly on cytotoxic immune effector cells, including natural killer (NK) cells, natural killer T (NKT) cells, and CD8$^+$ T cells, to stimulate their proliferation and increase their cytotoxic functions (12). IL12 also induces the differentiation of naïve T helper (Th) cells toward a Th1 phenotype and the production of cytokines (most notably IFNγ) that promote cell-mediated immunity (13). By amplifying these positive immunostimulatory effects, therapeutic administration of exogenous IL12 has the potential to promote effective antitumor immune responses.

Immuno-Oncology Translational Innovation Platform, EMD Serono Research and Development Institute, Billerica, Massachusetts.

Note: Supplementary data for this article are available at Clinical Cancer Research Online (http://clincancerres.aacrjournals.org/).

Corresponding Authors: Chunxiao Xu, EMD Serono Research and Development Institute, 45 Middlesex Turnpike, Billerica, MA 01821. Phone: 978-671-4745; E-mail: Chunxiao.xu@emdserono.com; and Yan Lan, yan.lan@emdserono.com

doi: 10.1158/1078-0432.CCR-17-0483

Translational Relevance

Anti-PD-1 and anti-PD-L1 immune checkpoint inhibitors have induced durable antitumor immune responses in patients with advanced-stage cancers; however, many patients do not benefit due to insufficient immune cell activation and infiltration into tumors. One approach to addressing this problem is through treatment with exogenous proinflammatory cytokines, such as IL12. Here, we show that a tumor-targeting murine IL12 fusion protein containing an anti-DNA antibody (NHS-muIL12), previously demonstrated to accumulate in necrotic areas within tumors, shows promising antitumor effects in combination with the anti-PD-L1 antibody avelumab. NHS-muIL12 synergized with avelumab to induce tumor regression, which was associated with enhanced immune cell infiltration and effector and memory T-cell development. Our findings indicate that NHS-muIL12 alters the tumor microenvironment by enhancing immune cell infiltration and sensitizing tumors to the effects of avelumab therapy, and support clinical trials assessing the combination of NHS-IL12 and avelumab for the treatment of solid tumors.

Intratumoral injection of IL12 in preclinical models was found to trigger a potent antitumor $CD8^+$ CTL response that regressed large, established tumors (14). However, initial clinical trials using systemically administered recombinant human IL12 were disappointing due to schedule-dependent toxicity mediated by high proinflammatory cytokine production (15). One way to minimize toxicity is to target IL12 to tumors via an antibody-cytokine fusion protein ("immunocytokine"). NHS-IL12 is a recombinant fusion protein consisting of the human monoclonal IgG1 antibody NHS76 fused at each CH_3 C-terminus to human IL12 (16). NHS76 targets exposed DNA, thereby directing the proinflammatory cytokine IL12 to intratumoral necrotic regions (17). NHS-IL12 was thus designed to alleviate the safety concerns associated with systemic administration of recombinant IL12 and to improve its pharmacokinetics (17). Indeed, NHS-IL12 treatment proved to be well-tolerated and showed preliminary evidence of clinical benefit in a phase I trial (NCT01417546).

Because human IL12 is not cross-reactive with the murine IL12 receptor, the chimeric surrogate immunocytokine NHS-muIL12, which consists of murine IL12 fused to the same human NHS76 antibody, was generated. NHS-muIL12 allows evaluation of the pharmacologic activity of the immunocytokine in immunocompetent tumor-bearing mice. In earlier studies, NHS-muIL12 accumulated in necrotic regions of tumors and exhibited superior tumor control relative to recombinant IL12 in multiple murine models (17). In this study, we evaluated the activity of NHS-muIL12 in combination with avelumab, a fully human anti-PD-L1 IgG1 antibody that binds to human and murine PD-L1 and blocks its interaction with PD-1 (18, 19). Avelumab has antitumor activity in murine tumor models and in clinical trials across multiple tumor indications, and was recently approved for treatment of Merkel cell carcinoma (20) and urothelial carcinoma (21). The data presented here demonstrate that the complementary immune-stimulatory effects of avelumab and NHS-muIL12 in combination enhanced antitumor activity over either treatment alone in two preclinical tumor models. A clinical trial evaluating combination therapy with NHS-IL12 and avelumab is currently being conducted (NCT02994953).

Materials and Methods

Mice

BALB/c mice were purchased from Charles River Laboratories and B6.129S2-Ighm^{tm1Cgn}/J (μMt^-) mice were purchased from Jackson Laboratory. All procedures were performed in accordance with institutional protocols approved by the Institutional Animal Care and Use Committee (IACUC) of EMD Serono Research and Development Institute.

Cell lines

EMT-6 and 4T1 breast cancer cell lines were obtained from the ATCC. The MC38 colon carcinoma cell line was provided by the Scripps Research Institute. All cell lines were tested and verified to be free of mycoplasma.

Treatments

The inactive anti-PD-L1 control (hereafter referred to as isotype control) is a mutated anti-PD-L1 antibody without the ability to bind PD-L1. Avelumab, isotype control, and NHS-muIL12 (17) were produced and purified at EMD Serono.

Murine tumor models

To generate the EMT-6 tumor model, BALB/c mice were inoculated with 0.5×10^6 EMT-6 tumor cells orthotopically in the mammary fat pad. To generate the MC38 tumor model, μMt^- mice were inoculated subcutaneously with 0.5×10^6 MC38 cells into the right flank.

Rechallenge with orthotopic mammary tumors. For tumor rechallenge studies, mice with complete remission of their EMT-6 tumors for over 3 months after the last treatment of NHS-muIL12 (2 or 10 μg) and avelumab (200 μg) combination therapy were injected with 1×10^6 EMT-6 tumor cells or 0.5×10^5 4T1 tumor cells into the opposite mammary pad from the original tumor site. As a control, naïve BALB/c mice were injected with tumor cells in the mammary pad.

In vivo treatments. Mice were randomized into treatment groups when tumors reached the desired volume (day 0) and treatment was initiated on day 0. Avelumab or isotype control were injected intravenously in 200 μL PBS on days 0, 3, and 6 for EMT-6 tumor–bearing mice and on days 0, 4, 7, 11, 14, 18, and 21 for MC38 tumor-bearing mice. NHS-muIL12 was injected as a single subcutaneous dose in 200 μL PBS on day 0.

ELISpot assay

ELISpot assay was performed to evaluate the frequency of IFNγ-producing $CD8^+$ T cells reactive to the tumor antigen p15E.

Flow cytometry

FACS staining was performed on dissociated spleens and tumors using standard procedures. FACS was performed on a MACSQuant® Analyzer 10, and quantified using FlowJo® software.

Immunohistochemistry

IHC was performed by Bioscience Solutions Group using the avidin–biotin complex (ABC) method. The following primary

antibodies were used: anti-mouse CD8 (Novus Biologicals, catalog no. AP-MAB0708) and anti-PD-L1 (Cell Signaling Technology, catalog no. 13684). Hematoxylin and eosin (H&E) staining was also performed.

NanoString® analysis

The NanoString® PanCancer Immune Profiling panel was used to evaluate whole tumor mRNA expression and R software was used to analyze data and generate plots. Background levels were calculated and subtracted from the samples, which were then normalized against the positive control and housekeeping gene probes. Normalized counts were analyzed using the default settings of DESeq2. Data are available in Gene Expression Omnibus (GEO) as accession number GSE93192. Heatmaps were produced with the pheatmap package and the sample order was set with a callback using optimal leaf ordering from the seriation package.

Plasma cytokine quantification by multiplex cytokine assay

Plasma cytokines were quantified at Eve Technologies Corp. using the Mouse Cytokine Array/Chemokine Array 32-Plex Assay Kit (Millipore) according to the manufacturers' instructions.

Plasma IFNγ quantification by ELISA

Plasma IFNγ was quantified using a mouse IFNγ Duoset ELISA Kit (R&D Systems, catalog no. DY485) following the manufacturer's instructions and read on a Synergy Biotek plate reader (Biotek).

Plasma kynurenine quantification by LC/MS-MS

Plasma kynurenine concentrations were determined by high-performance LC/MS-MS detection. The assay and analysis were performed at the Center for Analytical Services of Merck KGaA.

Statistical analysis

Line and bar graphs show mean and SEM; other graphs show data from individual mice (symbols) and means (horizontal line). Differences between treatment groups were determined by one- or two-way ANOVA followed by Bonferroni posttest. A Kaplan–Meier plot was generated to show survival by treatment group and significance was assessed by log-rank (Mantel–Cox) test. Analyses were performed using GraphPad Prism 6-7 and differences were determined to be significant if $P < 0.05$.

Additional details about procedures, culture conditions, and statistical analyses can be found in the Supplementary Materials and Methods.

Results

NHS-muIL12 and avelumab combination therapy enhanced antitumor efficacy relative to monotherapies and induced long-term protective immunity

To investigate the antitumor efficacy of combination therapy with NHS-muIL12 and avelumab, BALB/c mice bearing orthotopic EMT-6 tumors (~100 mm^3) were given a single subcutaneous dose of NHS-muIL12 (2 or 10 μg, day 0) alone or in combination with three intravenous doses (days 0, 3, 6) of avelumab (200 μg; $n = 8$ mice/group). NHS-muIL12 was administered subcutaneously because it is the method of administration being used in clinical studies with NHS-IL12. This was based on the preclinical finding that subcutaneous administration of NHS-muIL12 resulted in comparable levels of tumor uptake and reduced levels of liver uptake relative to intravenous administration, suggesting subcutaneous administration could have comparable efficacy with lower toxicity (17). An isotype control antibody was administered at the same dose and schedule as avelumab.

The higher dose of NHS-muIL12 (10 μg) significantly inhibited EMT-6 tumor growth compared with isotype control treatment (T/C = 35%; $P < 0.0001$; day 17; Fig. 1A and B). Although neither the lower dose of NHS-muIL12 (2 μg) (T/C = 73%, day 17) nor avelumab (200 μg) monotherapy (T/C = 62%, day 17) significantly inhibited tumor growth, combination of the two therapies elicited a synergistic antitumor effect (T/C = 6%, day 17) relative to either monotherapy ($P < 0.0001$ for both, day 17; Fig. 1A and B). Combination therapy with the higher dose of NHS-muIL12 and avelumab further inhibited tumor growth (T/C = 17%, day 17) relative to treatment with 10 μg NHS-muIL12 ($P = 0.0002$, day 17) or avelumab ($P < 0.0001$, day 17) alone (Fig. 1A and B).

The combination therapy with avelumab and NHS-muIL12 (2 or 10 μg) also prolonged survival in EMT-6 tumor-bearing mice [$P < 0.0001$, log-rank (Mantel–Cox) test; Fig. 1C]. Complete tumor regression was observed in 7 of 8 (88%) mice treated with either of the combination therapies (median survival >80 days), compared with 0/8 (0%) mice treated with isotype control (median survival = 17 days), 0/8 (0%) mice treated with 2 μg NHS-muIL12 (median survival = 20 days), 2/8 (25%) mice treated with 10 μg NHS-muIL12 (median survival = 33.5 days) and 1/8 (13%) mice treated with avelumab (median survival = 23 days; Fig. 1C).

A series of tumor rechallenge experiments were performed on mice that had displayed complete EMT-6 tumor regression for more than 3 months following combination therapy ("combination therapy-cured") to assess whether tumor-specific immune memory had been established. When combination therapy-cured mice ($n = 20$) were rechallenged with EMT-6 cells (subcutaneously), no tumor growth was observed, whereas naïve mice ($n = 8$) inoculated with EMT-6 cells rapidly developed tumors ($P < 0.0001$, day 28; Fig. 1D). However, combination therapy-cured mice ($n = 5$) challenged with 4T1 mammary tumor cells (subcutaneously) developed tumors at the same rate as naïve mice ($n = 8$; $P > 0.05$, day 28; Fig. 1D). Taken together, these data indicate that the combination therapy with NHS-muIL12 and avelumab induced the generation of tumor antigen–specific immune memory.

We next tested the antitumor efficacy of NHS-muIL12 and avelumab combination therapy in larger, more-established EMT-6 tumors (300–450 mm^3). Neither 0.5 μg NHS-muIL12 nor avelumab (200 μg) monotherapies inhibited tumor growth 8 days after treatment initiation, and treatment with 10 μg NHS-muIL12 only moderately decreased the mean tumor volume (32.2 ± 51.6 mm^3 decrease between days 0 and 8; $P > 0.05$; Supplementary Fig. S1A). In contrast, treatment with the combination of NHS-muIL12 (10 μg) and avelumab (200 μg) significantly reduced mean tumor volume (179.1 ± 86.5 mm^3 decrease between days 0 and 8; $P = 0.0385$; Supplementary Fig. S1A). In addition, tumor volume at day 8 was decreased in 6 of 8 mice (75%) after combination therapy with 10 μg NHS-muIL12 and avelumab, 2 of 8 mice (25%) after combination therapy with 0.5 μg NHS-muIL12 and avelumab, and 5 of 8 mice (62.5%) after 10 μg NHS-muIL12 monotherapy. Tumor regression was not observed in any of the mice treated with avelumab, NHS-muIL12 (0.5 μg), or the isotype control alone (Supplementary Fig. S1B).

The antitumor efficacy of the combination therapy was then evaluated in the MC38 colon carcinoma model in B-cell–deficient

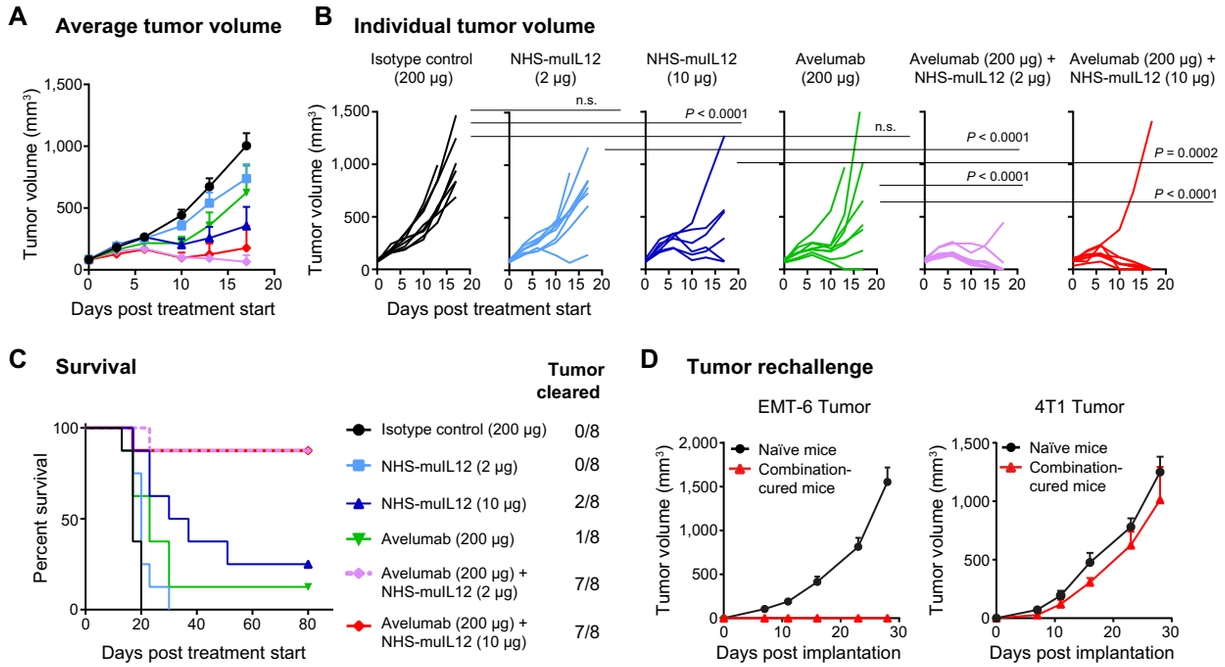

Figure 1.

NHS-muIL12 and avelumab combination treatment had a synergistic antitumor effect and induced long-term protective immunity in EMT-6 tumor–bearing mice. **A–C,** EMT-6 tumor–bearing BALB/c mice ($n = 8$ mice/group) were treated with: (i) isotype control (200 μg), (ii) NHS-muIL12 (2 μg), (iii) NHS-muIL12 (10 μg), (iv) avelumab (200 μg), (v) NHS-muIL12 (2 μg) + avelumab (200 μg), or (vi) NHS-muIL12 (10 μg) + avelumab (200 μg). NHS-muIL12 was injected as a single subcutaneous dose on day 0, and avelumab or isotype control were administered intravenously on days 0, 3, and 6. **A,** Average tumor volumes, measured twice weekly. Error bars represent SEM. **B,** Individual tumor volumes, in which each line represents a single mouse. *P* values were calculated by two-way ANOVA followed by Bonferonni posttest. **C,** Kaplan–Meier survival curve and proportion of tumor clearance in each treatment group. **D,** Mice in complete remission for 3 months following last combination treatment (mice from two repeat studies) and naïve BALB/c mice were challenged with EMT-6 ($n = 20$ and 8, respectively) or 4T1 ($n = 5$ and 8, respectively) cells by orthotopic injection on the opposite mammary pad of the original tumor site. Average tumor volume after implantation. Error bars represent SEM. n.s., not significant.

μMt$^-$ mice. Avelumab was administered on a repeat dosing schedule (400 μg, days 0, 4, 7, 11, 14, 18, and 21) to promote a sustained antitumor immune response. To prevent the induction of an immunogenic response to avelumab at this extended dosing schedule, B-cell–deficient mice were used. In these experiments, μMt$^-$ mice bearing subcutaneous MC38 tumors (~50 mm^3) were given a single dose of NHS-muIL12 alone (2 or 10 μg, day 0) or in combination with avelumab. The isotype control was administered at the same dose and schedule as avelumab. Tumor growth was not significantly inhibited by avelumab (T/C = 74%, day 21) or NHS-muIL12 (2 or 10 μg; T/C = 55% and 39%, respectively, day 21) monotherapies compared with isotype control (Fig. 2A and B). Combination treatment with avelumab and NHS-muIL12 (2 or 10 μg) enhanced antitumor efficacy (T/C = 19% and 10%, day 21) compared with avelumab ($P < 0.0001$ for both, day 21) and NHS-muIL12 ($P = 0.0006$ and 0.0001, respectively, day 21) monotherapies. Combination treatment with avelumab and NHS-muIL12 (2 or 10 μg) also extended survival in MC38 tumor-bearing mice (Fig. 2C), resulting in longer median survival times (35.5 and 36.5 days, respectively) than those of mice treated with avelumab (23.5 days) or NHS-muIL12 (2 μg or 10 μg; 28 and 29.5 days, respectively). The results in both EMT-6 and MC38 models demonstrate that combination treatment with NHS-muIL12 and avelumab is superior to either monotherapy in inhibiting tumor growth.

NHS-muIL12 and avelumab combination treatment elicited changes in immune phenotype in tumor-bearing mice

To further delineate the mechanism by which NHS-muIL12 and avelumab combination therapy enhanced antitumor activity, immune phenotypic signatures were determined via flow cytometry. In EMT-6 tumor-bearing BALB/c mice, NHS-muIL12 monotherapies enhanced proliferation of splenic NK and CD8$^+$ T cells in a dose-dependent manner (Fig. 3A). Combination treatment with NHS-muIL12 (10 μg) and avelumab further enhanced the proliferation of splenic NK and CD8$^+$ T cells relative to NHS-muIL12 ($P = 0.0125$ and $P = 0.0261$, respectively) or avelumab ($P < 0.0001$ and $P = 0.0347$, respectively) monotherapies (Fig. 3A). Similarly, in MC38 tumor-bearing μMt$^-$ mice, combination treatment with NHS-muIL12 (10 μg) and avelumab increased the percentage of proliferating CD8$^+$ T cells in the spleen ($P < 0.0001$) and tumor ($P = 0.0021$) relative to NHS-muIL12 monotherapy (Supplementary Fig. S2A).

In EMT-6 tumor-bearing mice, combination treatment with NHS-muIL12 (10 μg) and avelumab significantly increased splenic effector memory T (T_{EM}) cell frequency relative to NHS-muIL12 and avelumab monotherapies ($P = 0.0077$ and 0.0084, respectively) and trended toward an increase in splenic central memory T (T_{CM}) cell frequency (Fig. 3B). Similarly, in MC38 tumor-bearing mice, combination therapy increased splenic T_{EM} cell frequency relative to NHS-muIL12 ($P < 0.0001$) and avelumab

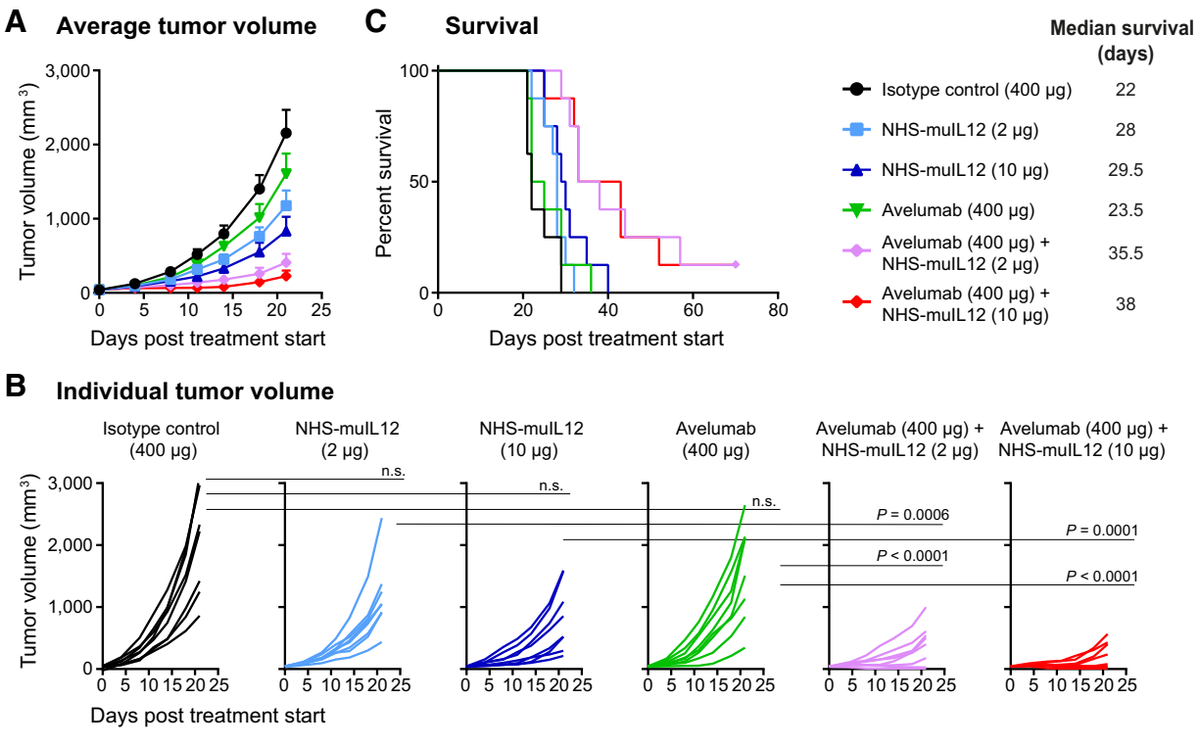

Figure 2.

NHS-muIL12 and avelumab combination treatment enhanced antitumor efficacy in MC38 tumor-bearing mice. **A–C**, MC38 tumor-bearing µMt$^-$ mice ($n = 8$ mice/group) were treated with: (i) isotype control (400 µg), (ii) NHS-muIL12 (2 µg), (iii) NHS-muIL12 (10 µg), (iv) avelumab (400 µg), (v) NHS-muIL12 (2 µg) + avelumab (400 µg), or (vi) NHS-muIL12 (10 µg) + avelumab (400 µg). NHS-muIL12 was administered subcutaneously on day 0, and avelumab and isotype control were administered intravenously on days 0, 4, 7, 11, 14, 18, and 21. **A,** Average tumor volumes, measured twice weekly. Error bars represent SEM. **B,** Individual tumor volumes; each line represents an individual mouse. *P* values were calculated by two-way ANOVA followed by Bonferonni posttest. **C,** Kaplan–Meier survival curve. Median survival times (days) are shown.

($P < 0.0001$) monotherapies, and showed a trend towards increasing T_{EM} cells in tumor relative to monotherapies (Supplementary Fig. S2B).

We next examined the effect of combination therapy on the expression of T-bet, a transcription factor involved in several immune functions, including CD8$^+$ T-cell differentiation and cytotoxicity, sustaining memory T-cell subsets, and NK-cell maturation (22, 23). NHS-muIL12 monotherapy increased the percentage of T-bet$^+$ NK cells and T-bet$^+$ CD8$^+$ T cells in the spleens of EMT-6 tumor–bearing BALB/c mice (Fig. 3C) and MC38 tumor–bearing µMt$^-$ mice (Supplementary Fig. S2C) in a dose-dependent manner. In EMT-6 tumor–bearing mice, combination therapy with NHS-muIL12 (10 µg) and avelumab significantly enhanced T-bet expression in NK and CD8$^+$ T cells relative to avelumab monotherapy ($P < 0.0001$, both) and in NK cells relative to NHS-muIL12 monotherapy ($P = 0.0090$; Fig. 3C). Similarly, in MC38 tumor-bearing mice, combination therapy (with 10 µg NHS-muIL12) significantly enhanced T-bet expression relative to avelumab in both spleen and tumor ($P = 0.0008$ and $P = 0.0435$), and relative to NHS-muIL12 in both spleen and tumor ($P < 0.0001$, both; Supplementary Fig. S2C).

Tumor-associated macrophages (TAM) play complex roles in tumorigenesis. The M1 (classically activated macrophage) subpopulation of TAMs highly expresses major histocompatibility complex class II (MHC II) and exerts antitumor effects through secretion of proinflammatory factors. The M2 (alternatively activated macrophage) subpopulation of TAMs has low MHC II expression and can promote the growth, invasion, and metastasis of tumors through the expression of inhibitory signaling molecules (24, 25). Combination of NHS-muIL12 (10 µg) and avelumab did not change MHC II^{low} or MHC II^{high} TAM frequency relative to NHS-muIL12 alone in EMT-6 (Fig. 3D) or MC38 tumor-bearing mice (Supplementary Fig. S2D). However, relative to avelumab, combination therapy decreased the frequency of MHC II^{low} macrophages ($P = 0.0002$) and increased the frequency of MHC II^{high} macrophages in the spleen ($P = 0.0008$) of EMT-6 tumor-bearing mice (Fig. 3D). Similarly, in MC38 tumor-bearing mice, combination therapy increased the frequency of MHC II^{high} macrophages relative to avelumab in both the spleen and tumor ($P < 0.0001$, both; Supplementary Fig. S2D). These results indicate that NHS-muIL12 was the main driver of the polarization towards an M1 TAM phenotype in the combination therapy with avelumab.

To evaluate tumor antigen-specific T-cell activation after combination therapy, we measured the response of splenic CD8$^+$ T cells from MC38 tumor-bearing mice to the murine tumor antigen

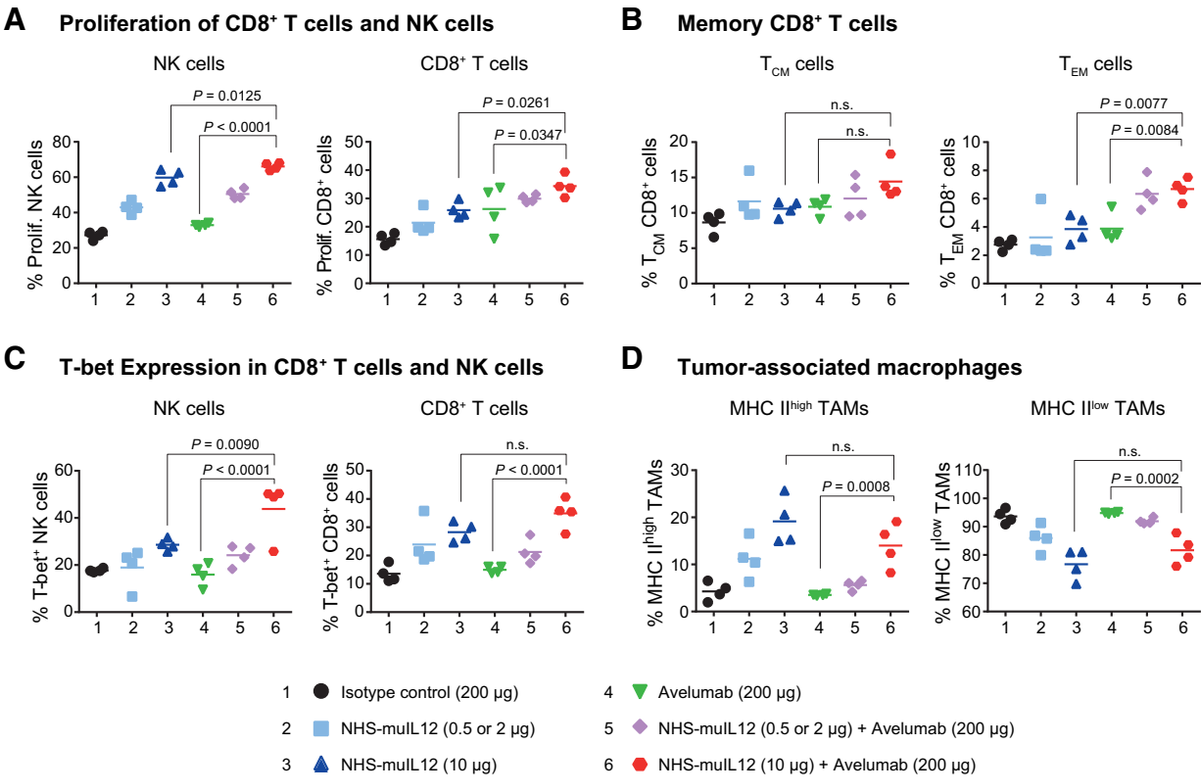

Figure 3.

Combination therapy with NHS-muIL12 and avelumab changed immune phenotypes. **A–D**, EMT-6 tumor-bearing BALB/c mice were treated ($n = 4$ mice/group) with one of the following: (i) isotype control (200 μg), (ii) NHS-muIL12 (2 μg for **A** and **B**; 0.5 μg for **C** and **D**), (iii) NHS-muIL12 (10 μg), (iv) avelumab (200 μg), (v) NHS-muIL12 (2 μg for **A** and **B**; 0.5 μg for **C** and **D**) + avelumab (200 μg), or (vi) NHS-muIL12 (10 μg) + avelumab (200 μg). FACS analysis of dissociated (**A–C**) spleens and (**D**) tumors harvested on day 5 after treatment initiation; percentages of gated cells are shown. **A,** Percentage of proliferating (Ki-67$^+$) splenic NK cells (CD49$^+$/DX5$^+$) and CD8$^+$ T cells (CD8$^+$/CD45$^+$). **B,** Percentage splenic central memory CD8$^+$ T cells (T_{CM}; CD44^{high}/CD62^{high}) and effector memory CD8$^+$ T cells (T_{EM}; CD44^{high}/CD62^{low}). **C,** Percentage T-bet$^+$ splenic NK cells and T-bet$^+$ CD8$^+$ T cells. **D,** Percentage MHC II^{high} or MHC II^{low} TAMs (CD45b$^+$/CD11b$^+$/Ly6C$^-$). *P* values were calculated using one-way ANOVA followed by Bonferroni posttest. n.s., not significant.

p15E (presented by antigen presenting cells) in ELISpot assays. Combination therapy with avelumab and NHS-muIL12 (2 or 10 μg) resulted in a synergistic increase in the frequency of p15E-reactive IFNγ-producing CD8$^+$ T cells relative to avelumab ($P < 0.0001$, both) and NHS-muIL12 ($P < 0.0001$, both; Supplementary Fig. S3A and B).

NHS-muIL12 treatment enhanced CD8$^+$ T-cell infiltration in tumors

We next asked whether the increase in splenic CD8$^+$ T-cell proliferation and maturation seen with NHS-muIL12 and avelumab combination treatment would translate to an increase in CD8$^+$ T-cell infiltration in EMT-6 orthotopic tumors. Tumor-bearing mice were treated with avelumab (200 μg, i.v.) on days 0 and 3, and/or NHS-muIL12 (2 μg or 10 μg, s.c.) on day 0. Immunohistochemical analysis of tumors showed that treatment with NHS-muIL12, alone or in combination with avelumab, dose-dependently increased CD8$^+$ T-cell infiltration in tumors relative to treatment with the isotype control (10 μg NHS-muIL12+avelumab: 26.1±7.7% CD8$^+$ cells; isotype control: 4.7±1.7% CD8$^+$ cells; $P = 0.0118$; Fig. 4A and B). However, there was no significant difference in infiltrated CD8$^+$ T-cell frequency between NHS-muIL12 monotherapy (10 μg) and combination therapy with NHS-muIL12 and avelumab, suggesting that the increase in CD8$^+$ T-cell infiltration was attributable to NHS-muIL12 therapy.

We next examined tumor-infiltrating lymphocytes (TIL) in H&E-stained EMT-6 tumor sections from mice treated with the isotype control. TILs were identified by their small, distinctive nuclear morphologies, and were found to surround, rather than infiltrate, areas of high tumor cell density (Supplementary Fig. S4A). IHC of matching sections demonstrated that TILs, but not tumor cells, expressed high levels of PD-L1 (Supplementary Fig. S4B). Furthermore, TIL "hotspots" were present within well-defined areas of focal necrosis, identified by the absence of stained tumor cell nuclei (Supplementary Fig. S4A). Both NHS-muIL12 (2 or 10 μg) and avelumab monotherapies increased the necrotic fraction of EMT-6 tumors relative to isotype control treatment (Supplementary Fig. S5). Combination treatment with NHS-muIL12 (2 or 10 μg) and avelumab further increased the necrotic fraction compared with either monotherapy (Supplementary Fig. S5), consistent with the enhanced tumor regression observed after combination therapy.

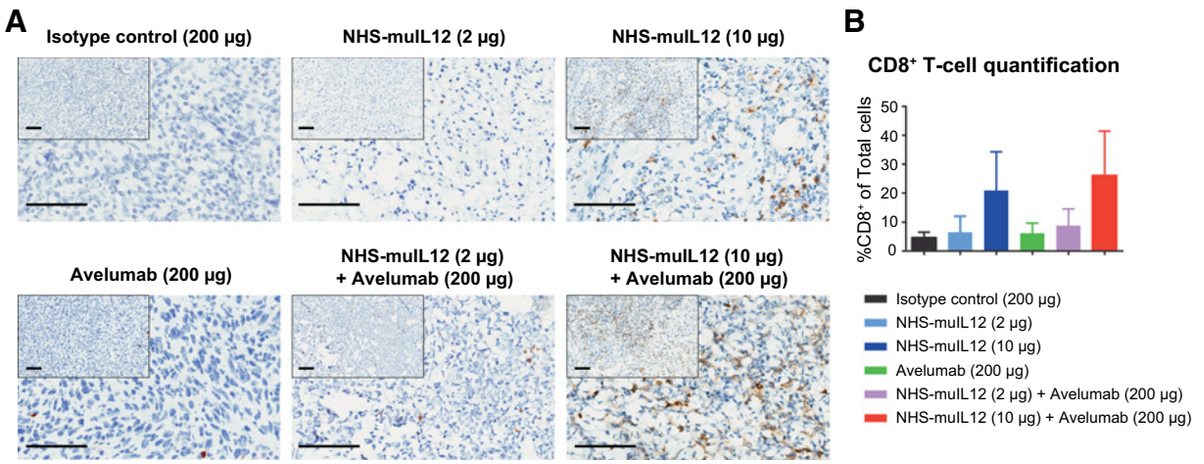

Figure 4.

NHS-muIL12 treatment enhanced CD8$^+$ T-cell infiltration in EMT-6 tumors. **A** and **B**: EMT-6 tumor-bearing mice were treated on day 0 ($n = 4$ mice/group) with: (i) isotype control (200 μg), (ii) NHS-muIL12 (2 μg), (iii) NHS-muIL12 (10 μg), (iv) avelumab (200 μg), (v) NHS-muIL12 (2 μg) + avelumab (200 μg), or (vi) NHS-muIL12 (10 μg) + avelumab (200 μg). Tumors were harvested on day 5, formalin fixed, and sectioned (5 μm) for anti-mouse CD8 antibody staining. **A,** Representative images of anti-CD8 IHC. Scale bars, 100 μm. **B,** Quantification of the average percentage of CD8$^+$ cells relative to total cells in tumors for each treatment group. Error bars represent SEM.

NHS-muIL12 and avelumab combination treatment elevated immune gene expression in the tumor and cytokine levels in the plasma

To further investigate the mechanism by which combination therapy enhanced antitumor efficacy, we examined immune-associated gene expression in the tumors and cytokine expression in the plasma of EMT-6 tumor–bearing mice treated with NHS-muIL12 and/or avelumab. Tumor mRNA was harvested 5 days after treatment initiation and immune gene expression was profiled by NanoString® PanCancer Immune Profiling Panels (see Supplementary Methods for data analysis protocol).

Compared with isotype control treatment, combination therapy with 10 μg NHS-muIL12 and avelumab (200 μg) resulted in differential expression (defined as $P < 0.05$ and log fold-change >1) of 138 of 770 genes evaluated. Combination therapy with the low dose of NHS-muIL12 induced nearly as many differentially expressed genes (120) relative to isotype control. In contrast, NHS-muIL12 monotherapy (2 and 10 μg) resulted in differential expression of only 7 and 45 genes, respectively, whereas avelumab monotherapy resulted in differential expression of only one gene. These data indicate that combination therapy elicited changes in expression of more genes than avelumab or NHS-muIL12 monotherapies (Fig. 5A).

A linear model analysis (26) accounting for both avelumab and NHS-muIL12 treatments was performed to determine their effects across all treatment groups. This analysis revealed that NHS-muIL12 contributed to the majority of gene expression changes observed after combination therapy with NHS-muIL12 and avelumab, particularly in genes that were upregulated (Fig. 5A, green boxes). The linear model analysis also showed that avelumab affected expression of a number of genes, primarily through downregulation of gene expression. Among the genes upregulated after NHS-muIL12 monotherapy or after combination therapy with NHS-muIL12 and avelumab were genes involved in innate and adaptive immune responses and cytokine and chemokine genes (Supplementary Fig. S6).

To determine which functional pathways were affected after combination therapy, Metacore pathway analysis was performed. Genes upregulated after combination therapy included those involved in leukocyte chemotaxis (e.g., *IP-10*, *MIG*), antigen presentation by MHC class II (e.g., *Cathepsin S*, *HLA-DRA1*), and Fc gamma receptor–mediated phagocytosis (e.g., *Fc gamma RI*, *Fc gamma RII alpha*; Supplementary Fig. S7). Combination therapy also upregulated expression of genes associated with IL10 signaling (e.g., *iNOS*, *IL10RA*), consistent with the known induction of IL10 by IL12 (27). Pathways with genes downregulated after combination therapy included those involved in naïve CD4$^+$ T-cell differentiation, particularly in Th17 differentiation and signaling (e.g., *IL17F*, *IL23*, *IL21*), consistent with previous reports showing that IL12 inhibits the development of Th17 cells (ref. 28; Supplementary Fig. S7).

Cancer immunotherapies have the potential to affect the expression of a broad range of cytokines downstream of their initial targets. These include Th1 cytokines, which promote antitumor activity through the activation of cytotoxic lymphocytes (CTL and NK cells; ref. 29), Th2 cytokines, which can induce a state of inflammation in the tumor microenvironment that has been associated with tumor tolerance (29), and chemokines, which can attract immune cells to the tumor. A multiplex cytokine assay was performed to monitor cytokine levels in plasma samples collected 2 days after treatment with a single dose of NHS-muIL12 (0.5 or 5 μg) alone or in combination with avelumab (200 μg) or isotype control (200 μg; Fig. 5B).

Combination treatment with NHS-muIL12 (5 μg) and avelumab (200 μg) enhanced levels of several cytokines compared with NHS-muIL12 (0.5 or 5 μg) or avelumab treatment alone (Fig. 5B). The combination therapy strongly induced the Th1 cytokine IFNγ, which is known to be potently induced by IL12 and is considered an important mediator of its antitumor activity (12), relative to NHS-muIL12 (5 μg) monotherapy (10.6-fold increase; $P < 0.0001$). Also increased relative to NHS-muIL12 was the proinflammatory cytokine TNFα, which

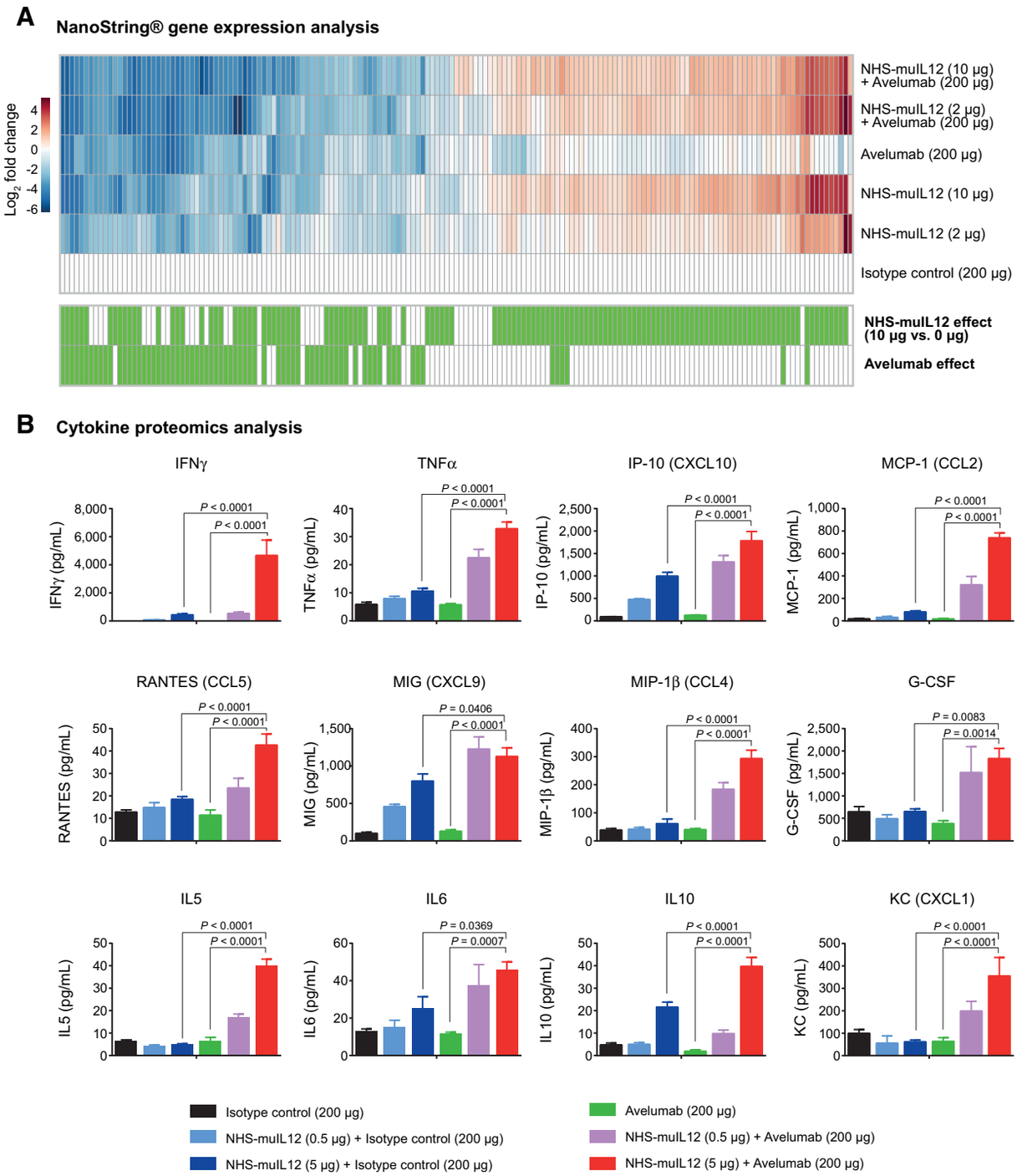

Figure 5.

NHS-muIL12 and avelumab combination treatment elevated gene expression in tumor tissue and cytokine levels in the plasma of the EMT-6 model. **A,** Heatmap of differentially expressed genes from a NanoString gene expression panel of mRNA from EMT-6 tumors ($n = 4$ mice/treatment) treated with one of the following: (G1) isotype control (200 μg), (G2) NHS-muIL12 (2 μg), (G3) NHS-muIL12 (10 μg), (G4) avelumab (200 μg), (G5) NHS-muIL12 (2 μg) + avelumab (200 μg), or (G6) NHS-muIL12 (10 μg) + avelumab (200 μg). The colors in each box in the heatmap represent the log2 fold-change in the median expression of a gene after treatment relative to isotype control. Each column represents a single gene. Genes were included in the heatmap if differential expression (defined as *P* value <0.05 and log-fold change >1) was identified in any of the following comparisons: G6 vs. G1, G5 vs. G3, G6 vs. G3, or G3 vs. G1. Green boxes (bottom) show significant effects of NHS-muIL12 and avelumab in a linear model that accounts for both across all treatment groups. **B,** Plasma concentrations of cytokines measured by Mouse Multiplex Cytokine Assay. EMT-6 tumor-bearing BALB/c mice were treated ($n = 5$ mice/group) on day 0 with single doses of (i) isotype control (200 μg), (ii) NHS-muIL12 (0.5 μg) + isotype control (200 μg), (iii) NHS-muIL12 (5 μg) + isotype control (200 μg), (iv) avelumab (200 μg), (v) NHS-muIL12 (0.5 μg) + avelumab (200 μg), or (vi) NHS-muIL12 (5 μg) + avelumab (200 μg). Blood samples were collected on day 2 and plasma concentrations of cytokines were measured. Error bars indicate SEM. *P* values were calculated using one-way ANOVA followed by Bonferroni posttest. n.s., not significant.

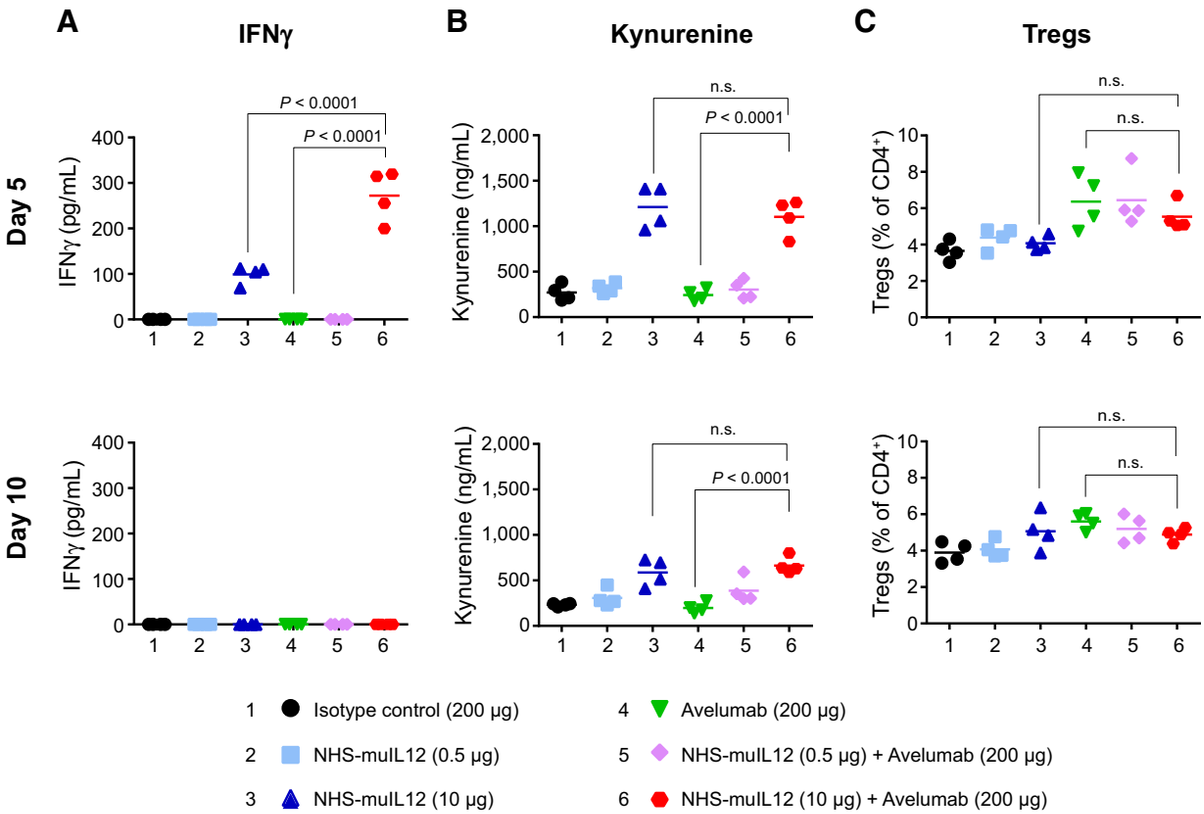

Figure 6.

NHS-muIL12 and avelumab combination treatment increased IFNγ but not kynurenine levels or the percentage of Treg cells relative to NHS-muIL12. **A–C,** EMT-6 tumor-bearing (~200–300 mm^3) mice were randomized ($n = 4$ mice/group) to one of the following treatments: (i) isotype control (200 μg), (ii) NHS-muIL12 (0.5 μg) + isotype control (200 μg), (iii) NHS-muIL12 (10 μg) + isotype control (200 μg), (iv) avelumab (200 μg), (v) NHS-muIL12 (0.5 μg) + avelumab (200 μg), or (vi) NHS-muIL12 (10 μg) + avelumab (200 μg). Isotype control and avelumab were injected intravenously on days 0 and 3, and NHS-muIL12 was injected subcutaneously on day 0. Blood samples and spleens were collected on day 5 and 10 after treatment initiation. **A,** IFNγ concentration in plasma, as determined by ELISA. **B,** Kynurenine concentration in plasma, as determined by high-performance LC/MS-MS. **C,** Flow cytometry of splenic Treg cells ($CD25^+$, $FoxP3^+$, $CD4^+$) as a percentage of $CD4^+$ splenocytes. Error bars indicate SEM. *P* values were calculated using one-way ANOVA followed by Bonferroni posttest. n.s., not significant.

mediates antitumor effects through damaging tumor vasculature and promoting T-cell and NK-cell cytotoxicity (3.1-fold increase; $P < 0.0001$; refs. 30, 31). The combination therapy also increased levels of Th2 cytokines, including IL5, IL6, and IL10, which have been associated with protumor inflammatory responses (32), relative to NHS-muIL12 alone (8.1-fold, 1.8-fold, and 1.8-fold increases, respectively; $P < 0.0001$, $P = 0.0369$, and $P < 0.0001$, respectively).

Chemokines involved in tumor inflammation were also upregulated in the plasma of mice following combination therapy with NHS-muIL12 and avelumab. For example, CXCL9 and CXCL10, which are known to be induced by IL12 (33), are involved in the chemotactic recruitment of CTLs and are considered to contribute to the antitumor effects of IL12 therapy through inhibition of tumor neovascularization (33). Combination therapy (with the high dose of NHS-muIL12) significantly increased both CXCL9 and CXCL10 plasma levels relative to NHS-muIL12 monotherapy (1.4- and 1.8-fold increase, respectively; $P = 0.0406$ and $P < 0.0001$, respectively; Fig. 5B).

NHS-muIL12 and avelumab combination treatment elevated IFNγ expression but did not significantly affect kynurenine levels or Treg percentages relative to NHS-muIL12 monotherapy

IFNγ is known to induce indoleamine 2,3-dioxygenase (IDO), an enzyme that inhibits antitumor responses through the depletion of the essential amino acid tryptophan and the production of its catabolite, kynurenine (Kyn; ref. 34). Increased Kyn levels appear to play an important role in the induction of Tregs and immune suppression (34, 35).

To investigate the potential effects of the combination therapy on this immunosuppressive pathway, we assessed IFNγ in the plasma of EMT-6 tumor–bearing mice 5 and 10 days after treatment with NHS-muIL12 (0.5 or 10 μg) and/or avelumab (200 μg). Avelumab did not significantly increase IFNγ levels, whereas NHS-muIL12 (10 μg) induced a moderate increase at day 5 ($P < 0.0001$). Combination therapy with NHS-muIL12 (10 μg) and avelumab markedly increased IFNγ levels relative to NHS-muIL12 (10 μg; $P < 0.0001$, 2.75-fold increase; Fig. 6A). By day 10, IFNγ was undetectable for all treatment groups.

Consistent with the induction of IFNγ, NHS-muIL12 (10 μg) treatment significantly increased Kyn levels at both day 5 and 10 relative to isotype control ($P < 0.0001$ and $P = 0.0004$, respectively). Combination therapy with 10 μg NHS-muIL12 and avelumab did not further increase Kyn levels compared with 10 μg NHS-muIL12 monotherapy (Fig. 6B), indicating that avelumab in the combination therapy does not contribute to further increases in Kyn levels.

Because Kyn accumulation can promote Treg differentiation, FACS was performed to determine the frequency of Tregs in the tumor. However, neither NHS-muIL12 (10 μg) or avelumab monotherapies, nor combination therapy with NHS-muIL12 and avelumab, significantly increased the percentage of Tregs on day 5 or 10 (Fig. 6C). These data show that although the combination therapy increased IFNγ levels relative to NHS-muIL12 (10 μg) monotherapy, it did not increase Kyn levels or the percentage of Tregs compared with NHS-muIL12 monotherapy.

Discussion

In this study, the antitumor efficacy of combination treatment with avelumab and NHS-muIL12 was investigated in murine tumor models. Treatment with NHS-muIL12 and avelumab elicited an enhanced antitumor effect relative to either monotherapy in both the EMT-6 model and the MC38 model. Most EMT-6 tumor-bearing mice treated with the combination therapy had complete tumor regression and developed tumor-specific immune memory, as demonstrated by their protection against rechallenge with EMT-6 tumor cells and the significant induction of effector and memory T cells. This is consistent with avelumab and NHS-muIL12 monotherapy–induced memory responses (17, 19).

Although anti-PD-1/PD-L1 monotherapies have shown durable antitumor effects in patients with advanced cancer, they are ineffective in certain patients due to a lack of immune cell infiltrates in the tumors. This represents a major obstacle to effective treatment with anti-PD-1/PD-L1 (36, 37). The combination treatment with NHS-muIL12 and avelumab dose-dependently stimulated cytotoxic NK and $CD8^+$ T-cell proliferation and induced $CD8^+$ T-cell infiltration into the tumor microenvironment, consistent with previous immune cell depletion studies demonstrating that the antitumor effects of NHS-muIL12 and avelumab monotherapies depend primarily on $CD8^+$ T cells (17, 19). Importantly, NHS-muIL12 treatment accounted for the majority of the $CD8^+$ T-cell infiltration seen in EMT-6 tumors after combination treatment, supporting the hypothesis that NHS-muIL12 therapy promotes a T-cell–inflamed tumor microenvironment that is more sensitive to avelumab therapy.

The strong induction of Th1 cytokines by the combination therapy with avelumab and NHS-muIL12 likely contributes to its potent antitumor activity. The Th1 cytokine IFNγ stimulates cytotoxic T-cell and NK-cell responses via STAT1 signaling, setting off a cascade of events that inhibit cell growth and promote tumor cell death (38). IFNγ also induces two key chemokines, CXCL10 and CXCL9, which drive effector $CD8^+$ T-cell migration into tumors via CXCR3 (39). Although IFNγ is known to be a key orchestrator of antitumor cellular immunity, the roles of other Th1 cytokines, such as TNFα, in mediating the antitumor effect of combination therapy with avelumab and NHS-muIL12 require further investigation. Recently, patients identified as nonresponders to immune checkpoint inhibitors were found to harbor tumors with genomic defects in IFNγ and STAT1 signaling pathways (40). One outstanding question is the degree to which IL12 therapy, alone or in combination with avelumab, is dependent on IFNγ and STAT1 signaling, and whether the combination therapy can be as effective in patients with deficits in IFNγ-STAT1 signaling.

In addition to inducing IFNγ and other Th1 cytokines, NHS-muIL12, alone and in combination with avelumab, induced Th2 cytokines, such as IL10 and IL5. Although IL12 therapy has been shown to strongly promote the release of Th1 cytokines, particularly IFNγ, it is also known to self-limit excessive proinflammatory activity through the induction of immunosuppressive Th2 cytokines, such as IL10, which limit the immune response to prevent damage to the host (29, 32, 41). However, IL10 also has an emerging role in driving anti-tumor effector $CD8^+$ T-cell responses (42, 43). Indeed, IL10 was recently found to enhance the survival and effector function of tumor-infiltrating $CD8^+$ T cells by enhancing IFNγ and MHC class I expression in tumors through a STAT3-mediated mechanism (42, 43) and, along with IL21, was found to induce central memory $CD8^+$ T-cell differentiation (44). IL10 has also been shown to synergize with IL12 to enhance survival in tumor-bearing mice when both cytokines are administered in combination (45). Thus, the induction of both Th1 cytokines and Th2 cytokines by NHS-muIL12 and avelumab combination therapy may not only represent an important balance between the antitumor immune response and the prevention of damaging autoimmunity, but may induce a multifaceted positive feedback response reinforcing differentiated $CD8^+$ CTL responses at the tumor site.

Another consideration in IL12 treatment and T-cell checkpoint blockade is the role of increased IDO activity as a potential mechanism of adaptive resistance. IDO catabolizes tryptophan in the tumor microenvironment, leading to accumulation of Kyn and its metabolites (46). The data presented here show that NHS-muIL12, alone or in combination with avelumab, induced an increase in plasma Kyn levels, indicating induction of IDO, which is an IFNγ-induced gene (47). IDO serves as an anti-inflammatory signaling system that limits potentially damaging autoimmune responses in part through the induction of tolerogenic dendritic cells (DC) that induce Treg expansion (48). These IDO-mediated events may self-limit the proinflammatory effects of IL12 (49). However, although NHS-muIL12 drove Kyn accumulation in our tumor models, combining NHS-muIL12 with avelumab did not further increase plasma Kyn levels, nor did it increase the percentage of immunosuppressive Tregs relative to NHS-muIL12 alone. These findings suggest that blockade of PD-L1 does not exacerbate IDO-driven negative feedback effects of IL12.

In summary, our preclinical data demonstrate that NHS-muIL12 alters the tumor microenvironment by increasing the infiltration of immune cells to enhance immunogenicity. Thus, NHS-IL12 may switch a less T-cell–inflamed "cold" tumor to an immune-responsive, more T-cell–inflamed "hot" tumor, and thereby render the tumor more sensitive to the effects of avelumab treatment. These findings support a combination immunotherapy of NHS-IL12 and avelumab in clinical trials for the treatment of solid tumors.

Disclosure of Potential Conflicts of Interest

P. Alexander Rolfe is employed at the EMD Serono Research and Development Institute. J.M English is a VP Head of Discovery TIP

Immuno-Oncology at the EMD Serono Research and Development Institute. No potential conflicts of interest were disclosed by the other authors.

Authors' Contributions

Conception and design: C. Xu, R. Tighe, K.-M. Lo, J.M. English, Y. Lan
Development of methodology: C. Xu, Y. Zhang, B. Marelli, G. Qin, J. Qi, H. Wang, H. Yu
Acquisition of data (provided animals, acquired and managed patients, provided facilities, etc.): C. Xu, Y. Zhang, W. Guzman, G. Kradjian, B. Marelli, G. Qin, J. Qi, H. Wang, H. Yu
Analysis and interpretation of data (e.g., statistical analysis, biostatistics, computational analysis): C. Xu, Y. Zhang, P. Alexander Rolfe, V.M. Hernández, W. Guzman, G. Kradjian, B. Marelli, G. Qin, J. Qi, H. Wang, H. Yu, L. Radvanyi
Writing, review, and/or revision of the manuscript: C. Xu, P. Alexander Rolfe, V.M. Hernández, R. Tighe, K.-M. Lo, J.M. English, L. Radvanyi, Y. Lan
Administrative, technical, or material support (i.e., reporting or organizing data, constructing databases): C. Xu, B. Marelli, G. Qin, J. Qi, H. Yu
Study supervision: C. Xu, W. Guzman, R. Tighe, J.M. English, L. Radvanyi, Y. Lan

Acknowledgments

The authors would like to thank Molly Jenkins for assistance with manuscript preparations and the Center for Analytical Services of Merck KGaA for determining the concentrations of Kyn via LC-MS.

Grant Support

This study was sponsored by Merck KGaA. Avelumab is being developed through an alliance between Merck KGaA and Pfizer, Inc.

The costs of publication of this article were defrayed in part by the payment of page charges. This article must therefore be hereby marked *advertisement* in accordance with 18 U.S.C. Section 1734 solely to indicate this fact.

Received February 17, 2017; revised June 2, 2017; accepted June 29, 2017; published OnlineFirst July 5, 2017.

References

1. Li Y, Li F, Jiang F, Lv X, Zhang R, Lu A, et al. A mini-review for cancer immunotherapy: molecular understanding of PD-1/PD-L1 pathway & translational blockade of immune checkpoints. Int J Mol Sci 2016;17:1151–73.
2. Chen J, Jiang CC, Jin L, Zhang XD. Regulation of PD-L1: a novel role of pro-survival signalling in cancer. Ann Oncol 2016;27:409–16.
3. Dong H, Strome SE, Salomao DR, Tamura H, Hirano F, Flies DB, et al. Tumor-associated B7-H1 promotes T-cell apoptosis: a potential mechanism of immune evasion. Nat Med 2002;8:793–800.
4. Chen DS, Irving BA, Hodi FS. Molecular pathways: next-generation immunotherapy–inhibiting programmed death-ligand 1 and programmed death-1. Clin Cancer Res 2012;18:6580–7.
5. Weber JS, D'Angelo SP, Minor D, Hodi FS, Gutzmer R, Neyns B, et al. Nivolumab versus chemotherapy in patients with advanced melanoma who progressed after anti-CTLA-4 treatment (CheckMate 037): a randomised, controlled, open-label, phase 3 trial. Lancet Oncol 2015;16:375–84.
6. Robert C, Schachter J, Long GV, Arance A, Grob JJ, Mortier L, et al. Pembrolizumab versus ipilimumab in advanced melanoma. N Engl J Med 2015;372:2521–32.
7. Borghaei H, Paz-Ares L, Horn L, Spigel DR, Steins M, Ready NE, et al. Nivolumab versus docetaxel in advanced nonsquamous non-small-cell lung cancer. N Engl J Med 2015;373:1627–39.
8. Fehrenbacher L, Spira A, Ballinger M, Kowanetz M, Vansteenkiste J, Mazieres J, et al. Atezolizumab versus docetaxel for patients with previously treated non-small-cell lung cancer (POPLAR): a multicentre, open-label, phase 2 randomised controlled trial. Lancet 2016;387:1837–46.
9. Nghiem PT, Bhatia S, Lipson EJ, Kudchadkar RR, Miller NJ, Annamalai L, et al. PD-1 blockade with pembrolizumab in advanced merkel-cell carcinoma. N Engl J Med 2016;374:2542–52.
10. Galon J, Pages F, Marincola FM, Angell HK, Thurin M, Lugli A, et al. Cancer classification using the immunoscore: a worldwide task force. J Translat Med 2012;10:205.
11. Kim J, Heery C, Bilusic M, Singh N, Madan R, Sabzevari H, et al. First-in-human phase I trial of NHS-IL12 in advanced solid tumors. ASCO Annual Meeting Proceedings 2012;30:TPS2617.
12. Del Vecchio M, Bajetta E, Canova S, Lotze MT, Wesa A, Parmiani G, et al. Interleukin-12: biological properties and clinical application. Clin Cancer Res 2007;13:4677–85.
13. Athie-Morales V, Smits HH, Cantrell DA, Hilkens CM. Sustained IL-12 signaling is required for Th1 development. J Immunol 2004;172:61–9.
14. Zaharoff DA, Hance KW, Rogers CJ, Schlom J, Greiner JW. Intratumoral immunotherapy of established solid tumors with chitosan/IL-12. J Immunother 2010;33:697–705.
15. Haicheur N, Escudier B, Dorval T, Negrier S, De Mulder PH, Dupuy JM, et al. Cytokines and soluble cytokine receptor induction after IL-12 administration in cancer patients. Clin Exp Immunol 2000;119:28–37.
16. Gillies SD, Lan Y, Wesolowski JS, Qian X, Reisfeld RA, Holden S, et al. Antibody-IL-12 fusion proteins are effective in SCID mouse models of prostate and colon carcinoma metastases. J Immunol 1998;160:6195–203.
17. Fallon J, Tighe R, Kradjian G, Guzman W, Bernhardt A, Neuteboom B, et al. The immunocytokine NHS-IL12 as a potential cancer therapeutic. Oncotarget 2014;5:1869–84.
18. Fallon JK, Vandeveer AJ, Schlom J, Greiner JW. Enhanced antitumor effects by combining an IL-12/anti-DNA fusion protein with avelumab, an anti-PD-L1 antibody. Oncotarget 2017;8:20558–71.
19. Vandeveer AJ, Fallon JK, Tighe R, Sabzevari H, Schlom J, Greiner JW. Systemic immunotherapy of non-muscle invasive mouse bladder cancer with avelumab, an anti-PD-L1 Immune checkpoint inhibitor. Cancer Immunol Res 2016;4:452–62.
20. Kaufman HL, Russell J, Hamid O, Bhatia S, Terheyden P, D'Angelo SP, et al. Avelumab in patients with chemotherapy-refractory metastatic Merkel cell carcinoma: a multicentre, single-group, open-label, phase 2 trial. Lancet Oncol 2016;17:1374–85.
21. Farina MS, Lundgren KT, Bellmunt J. Immunotherapy in urothelial cancer: recent results and future perspectives. Drugs 2017;77:1077–89.
22. Knox JJ, Cosma GL, Betts MR, McLane LM. Characterization of T-bet and eomes in peripheral human immune cells. Front Immunol 2014;5:217.
23. Lazarevic V, Glimcher LH, Lord GM. T-bet: a bridge between innate and adaptive immunity. Nat Rev Immunol 2013;13:777–89.
24. Ruffell B, Affara NI, Coussens LM. Differential macrophage programming in the tumor microenvironment. Trends Immunol 2012;33:119–26.
25. Mills CD, Lenz LL, Harris RA. A breakthrough: macrophage-directed cancer immunotherapy. Cancer Res 2016;76:513–6.
26. Love MI, Huber W, Anders S. Moderated estimation of fold change and dispersion for RNA-seq data with DESeq2. Genome Biol 2014;15:550.
27. Meyaard L, Hovenkamp E, Otto SA, Miedema F. IL-12-induced IL-10 production by human T cells as a negative feedback for IL-12-induced immune responses. J Immunol 1996;156:2776–82.
28. Cornelissen F, van Hamburg JP, Lubberts E. The IL-12/IL-23 axis and its role in Th17 cell development, pathology and plasticity in arthritis. Curr Opin Investig Drugs 2009;10:452–62.
29. Burkholder B, Huang RY, Burgess R, Luo S, Jones VS, Zhang W, et al. Tumor-induced perturbations of cytokines and immune cell networks. Biochim Biophys Acta 2014;1845:182–201.
30. Balkwill F. Tumor necrosis factor or tumor promoting factor? Cytokine Growth Factor Rev 2002;13:135–41.
31. Roberts NJ, Zhou S, Diaz LA Jr, Holdhoff M. Systemic use of tumor necrosis factor alpha as an anticancer agent. Oncotarget 2011;2:739–51.
32. Johansson M, Denardo DG, Coussens LM. Polarized immune responses differentially regulate cancer development. Immunol Rev 2008;222:145–54.
33. Kanegane C, Sgadari C, Kanegane H, Teruya-Feldstein J, Yao L, Gupta G, et al. Contribution of the CXC chemokines IP-10 and Mig to the antitumor effects of IL-12. J Leukocyte Biol 1998;64:384–92.

34. Prendergast GC. Immune escape as a fundamental trait of cancer: focus on IDO. Oncogene 2008;27:3889–900.
35. Fallarino F, Grohmann U, You S, McGrath BC, Cavener DR, Vacca C, et al. The combined effects of tryptophan starvation and tryptophan catabolites down-regulate T cell receptor zeta-chain and induce a regulatory phenotype in naive T cells. J Immunol 2006;176:6752–61.
36. Daud AI, Loo K, Pauli ML, Sanchez-Rodriguez R, Sandoval PM, Taravati K, et al. Tumor immune profiling predicts response to anti-PD-1 therapy in human melanoma. J Clin Invest 2016;126:3447–52.
37. Tang H, Wang Y, Chlewicki LK, Zhang Y, Guo J, Liang W, et al. Facilitating T cell infiltration in tumor microenvironment overcomes resistance to PD-L1 blockade. Cancer Cell 2016;30:500.
38. Ikeda H, Old LJ, Schreiber RD. The roles of IFN gamma in protection against tumor development and cancer immunoediting. Cytokine Growth Factor Rev 2002;13:95–109.
39. Billottet C, Quemener C, Bikfalvi A. CXCR3, a double-edged sword in tumor progression and angiogenesis. Biochim Biophys Acta 2013; 1836:287–95.
40. Gao J, Shi LZ, Zhao H, Chen J, Xiong L, He Q, et al. Loss of IFN-gamma pathway genes in tumor cells as a mechanism of resistance to anti-CTLA-4 therapy. Cell 2016;167:397–404.
41. de Vries JE. Immunosuppressive and anti-inflammatory properties of interleukin 10. Ann Med 1995;27:537–41.
42. Mumm JB, Emmerich J, Zhang X, Chan I, Wu L, Mauze S, et al. IL-10 elicits IFNgamma-dependent tumor immune surveillance. Cancer Cell 2011;20: 781–96.
43. Oft M.IL-10: master switch from tumor-promoting inflammation to anti-tumor immunity. Cancer Immunol Res 2014;2:194–9.
44. Cui W, Liu Y, Weinstein JS, Craft J, Kaech SM. An interleukin-21-interleukin-10-STAT3 pathway is critical for functional maturation of memory CD8+ T cells. Immunity 2011;35:792–805.
45. Lopez MV, Adris SK, Bravo AI, Chernajovsky Y, Podhajcer OL. IL-12 and IL-10 expression synergize to induce the immune-mediated eradication of established colon and mammary tumors and lung metastasis. J Immunol 2005;175:5885–94.
46. Selvan SR, Dowling JP, Kelly WK, Lin J. Indoleamine 2,3-dioxygenase (IDO): biology and target in cancer immunotherapies. Curr Cancer Drug Targets 2016;16:755–64.
47. Taylor MW, Feng GS. Relationship between interferon-gamma, indoleamine 2,3-dioxygenase, and tryptophan catabolism. FASEB J 1991; 5:2516–22.
48. Mellor AL, Munn DH. IDO expression by dendritic cells: tolerance and tryptophan catabolism. Nat Rev Immunol 2004;4:762–74.
49. Li Q, Virtuoso LP, Anderson CD, Egilmez NK. Regulatory rebound in IL-12-treated tumors is driven by uncommitted peripheral regulatory T cells. J Immunol 2015;195:1293–300.